Novel, Broadband, Material Independent Luminescence Enhancement Technique Based on Surface Texturing

Noha S. A.
The American University in Cairo, Egypt, noha.abouqara@gmail.com, nohaaboqara@aucegypt.edu

Abstract-Upconverting nanoparticles (UCNPs) have been of crucial significance in multiple applications involving photochemical, biomedical and optical ones. For the biomedical applications, one main problem that always stands as a challenge, hindering the upconversion scheme from being deployed inside human cells, is the challenging trade-offs among biomedical and field enhancement requirements imposed by the biomedical design constraints that deprive the UCNPs from field enhancement. Another challenge is imposed due to the constraint on the material choice that should achieve the required targeting, treatment/imaging, and electromagnetic design objective without any harm threatening the human body, which involves the dose limited by biodegradability and biocompatibility of the material. Although multiple field enhancement and manipulation techniques have been applied to UCNPs, there has never been a generic, material independent field enhancement method that could be invoked in biomedical applications without harming the human body despite achieving the required dose. This is a global transformation in the field of photoluminescence (PL) enhancement where there are constraints in the material, specially in biomedical applications, which has been the focus of this numerical and theoretical work. Besides, a more concrete explanation had to be provided to fit the practically obtained results that do not go in line with the conventional perception of electromagnetic waves guidance and confinement in nanostructures.

Keywords: Upconverting Nanoparticles, field enhancement, surface texturing, moth-eye

I. INTRODUCTION:

Based on the literature review done before [1], the only two feasible approaches for field enhancement are the material based and the surface texturing ones. While the material dependent one is exhausted in a prior work [2], this approach is still problematic in multiple applications where the several constraints on the material make it inapplicable. Thus, this leads us to think of another material independent approach. Surface texturing is one approach that could resolve this problem through increasing the anti-reflectivity and thus increasing the incident intensity to the core layer and has been introduced in the prior work referred to. This is crucial for the direct correlation between the output PL and the incident excitation intensity shown in all literature studies focusing on lanthanide doped UCNPs.

Various studies have turned attention to moth eye structures as promising antireflective coatings for a broad range of applications. Many studies have been dedicated to the fabrication process [3], [4] , [5], [6], [7], [8], [9] fitting it into solar cell or other applications [10], [11], [12], [13], [14], [15], [16] or optimizing the geometric parameters of the structure [17], [18], [19], [20], [21], [22], [23]. Other works have explained the general antireflection principles derived from previously published work in this field [24]. One promising, novel line of thought is the concept of self-similarity could suggest new and complement existing dimensions of thinking about moth eye antireflectivity due to the conventional perception of gradually leading the incident excitation through a gradual spacial change in the coating [25], [26], [27]. However, this concept has been disproved in this work based on our numerical studies. Thus, a more concrete explanation has to be provided.

II. MATERIALS, METHODS AND RESULTS:

A) Theoretical Assumptions:

The idea is based on minimizing the reflection and diffraction taking place on the grating/input medium interface which may be the reason for low coupling. Instead of the sharp, periodic discontinuous grating structure, we can make it smooth so that the incident light sees it as if it's one effective medium. This gradual confinement of light may happen if the light sees the overall structure far away from the surface, the same as it sees it in proximity.

We found that cos (ax)* cos (b x), where a<b, has an envelope is also a cosine function as shown below. i.e., the same functional variation happens at the overall (blue envelope) surface seen far away by the light and in proximity (the red cos function). Thus, this is how self-similarity can be interpreted in a mathematical sense.

The values of a and b will be pending the application. The core nanoparticles size would limit the number of domes on it and thus the value of b. The value of a is bounded by the nanoparticles obtainable size as well. Besides, these parameters can be optimized in the frame of practically obtained results.

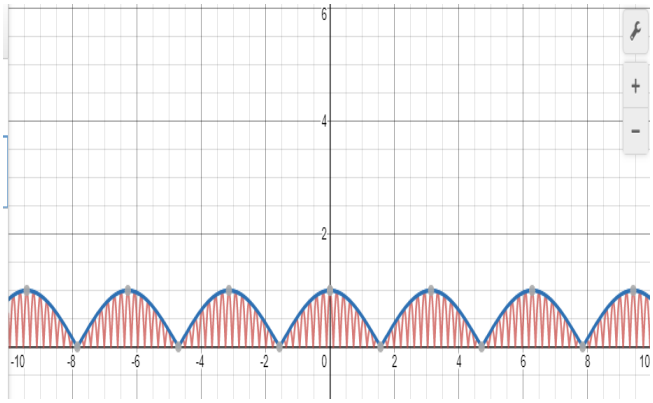

Figure (1): proposed structure front view. The figure is drawn using Desmos graphing tool.

B) Design Parameters:

Refractive Index=1.4 [varied later]

Size: infinite substrate, the dimensions of the protrusions and their separations are varied

Boundary Conditions: Perfectly Matched Layers in the vertical direction, symmetric and antisymmetric in the horizontal plane to minimize the computational complexity.

Background: was varied from air to blood, to mimic the application situation.

Source: plane wave, broadband from .1-2 um

Mesh Accuracy: 7

Simulation time: 4000 fs and was varied in several iterations from 1000 to 5000 to make sure it won't introduce any numerical errors.

Auto Shut-off level and dt stability were adjusted so as to converge.

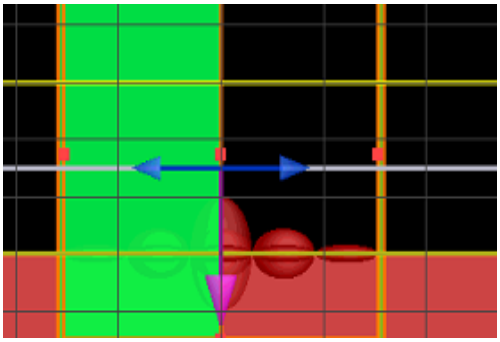

Figure (2): The Initially Simulated Design

C) Implementation

*Color Code:

Throughout measurements, the reflectance is in green and transmission is in blue

*Nomenclature: The envelope is the envelope function, representing the cosine function of lower frequency. The small structures refer to the structures embodying the cosine function of higher frequency.

1-Setting up a control measurement:

In this step, we measured the reflection and transmission of the flat substrate of the material to have a reference with which we can compare the effect of surface texturing. In addition, the reflection and transmission of each of the envelopes, small structures and self-similar structures are measured.

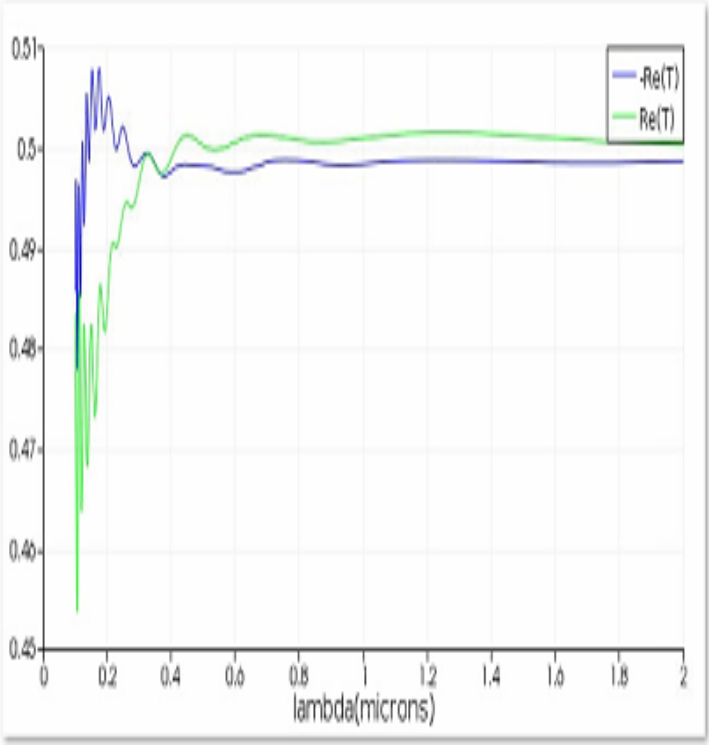

Figure (3) shows the reflection and transmission of a flat surface

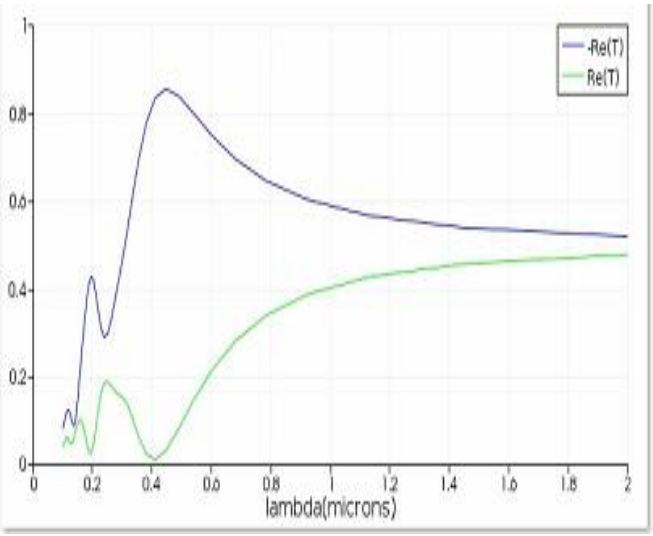

Figure (4) shows the reflection and transmission of the of small structure

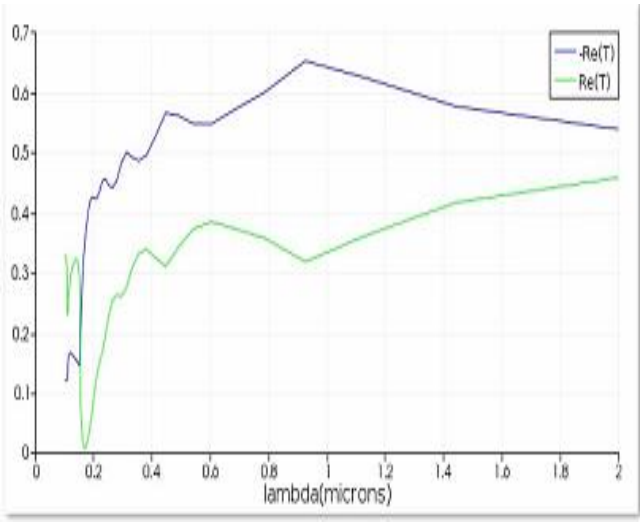

Figure (5) shows the reflection and transmission of the envelope only.

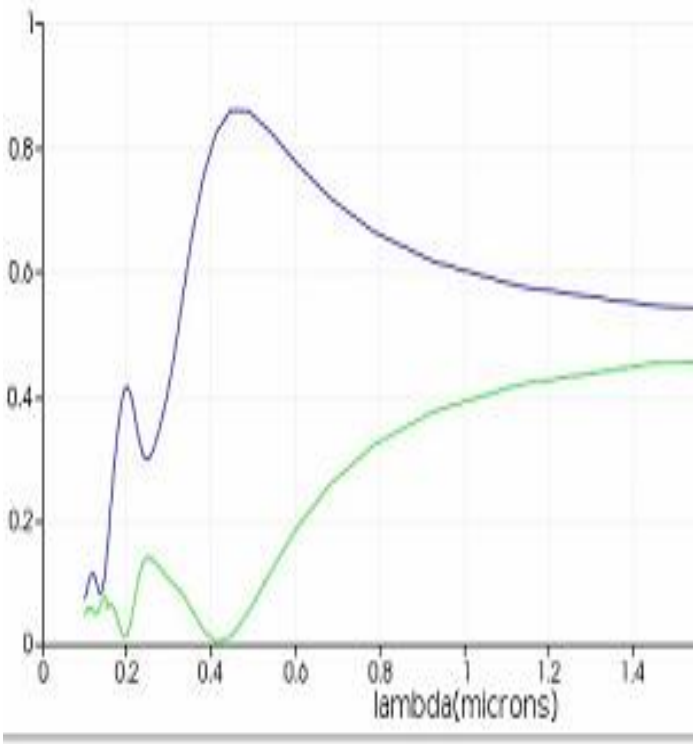

Figure (6) shows the reflection and transmission of the self-similar structure

2-Parameters variation:

In this step, the objective was to find the optimum dimensions that minimize the reflection. In addition, we aimed at finding the pattern that represents the key in minimizing surface texturing.

I) Height:

At this point, we increased the height of both self-similar structures, the envelope and the small structures separately. Furthermore, the envelope shape (frequency) was also changed to further investigate if this persistent effect of height increase would remain.

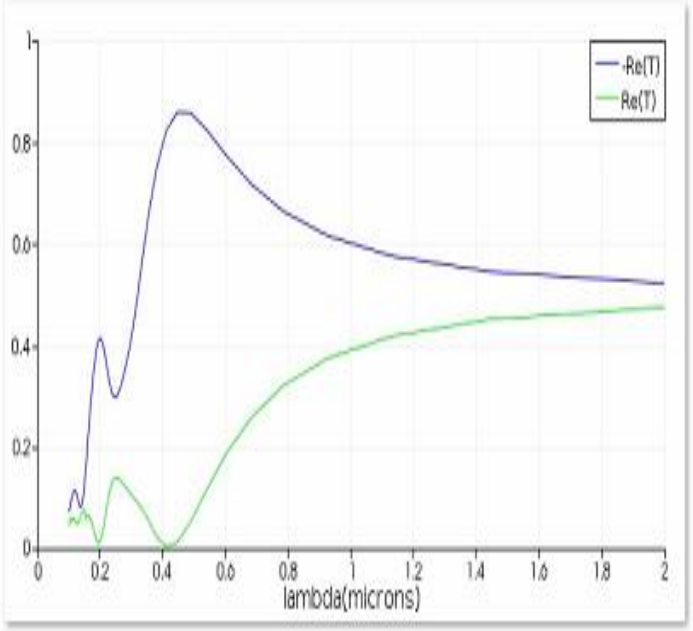

Figure (7) shows the reflection and transmission of the short self-similar structures

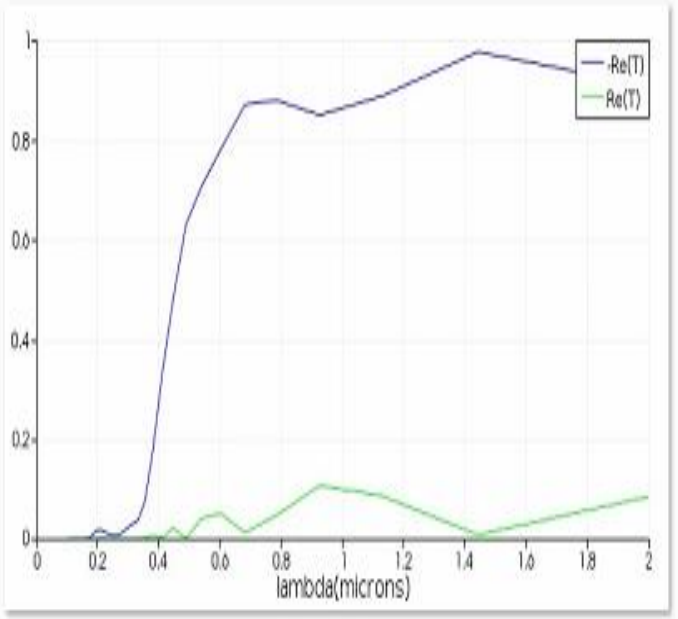

Figure (8) shows the reflection and transmission of the tall self-similar structures

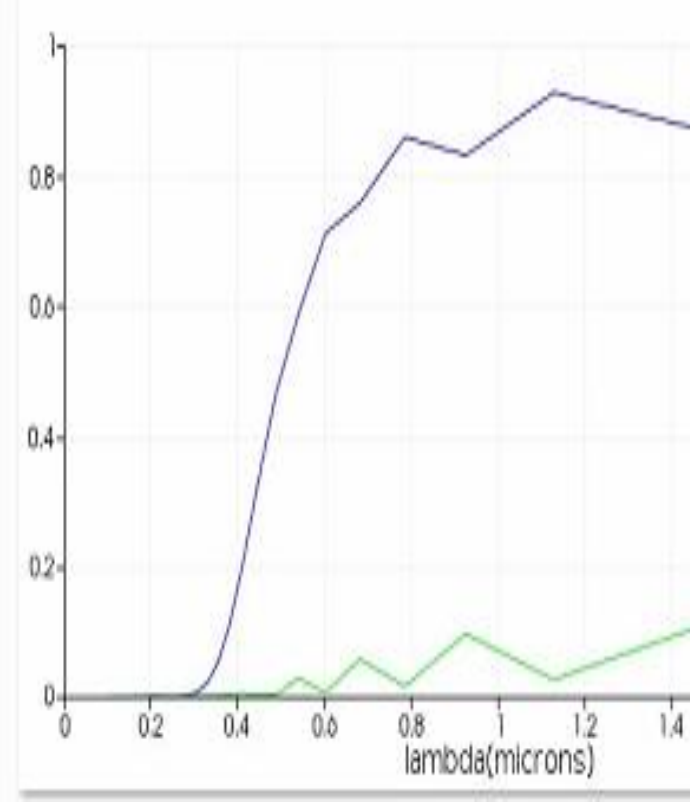

Figure (9) shows the reflection and transmission of the small structures upon increasing the height

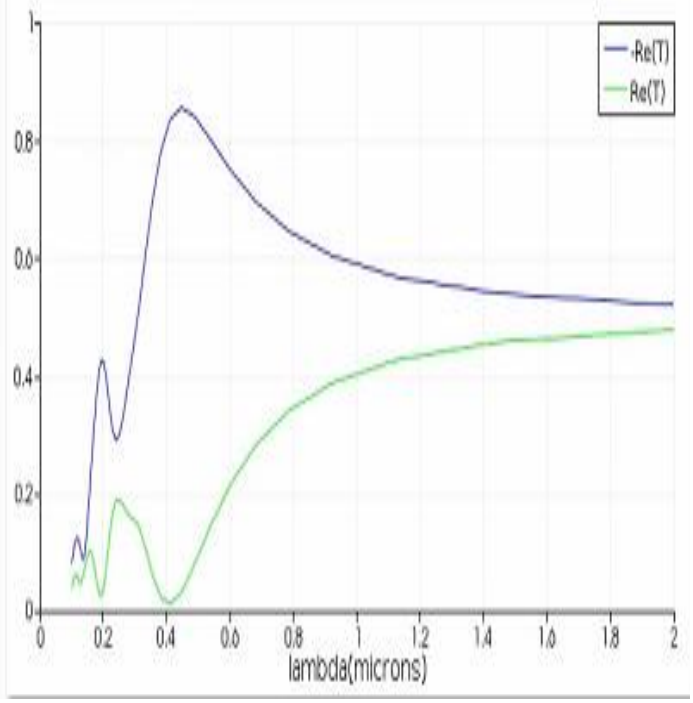

Figure (10) shows the reflection and transmission of the small structures before increasing the height.

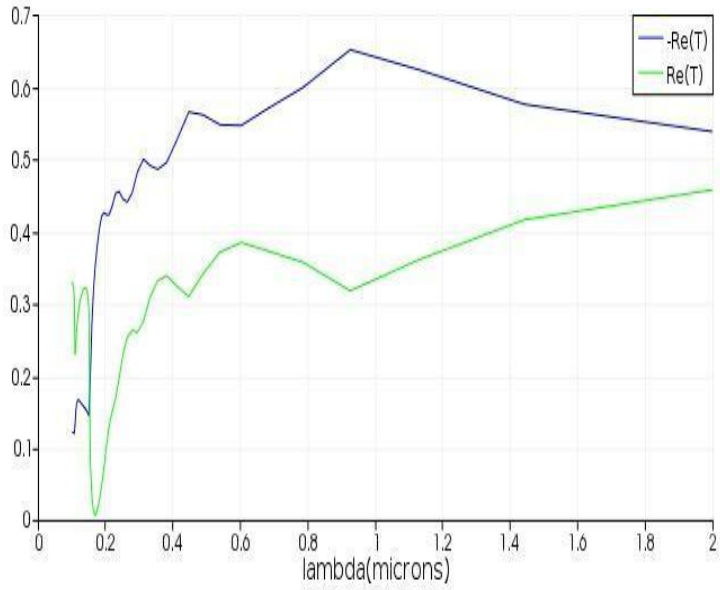

Figure (11) shows the reflection and transmission of the envelope before increasing the height.

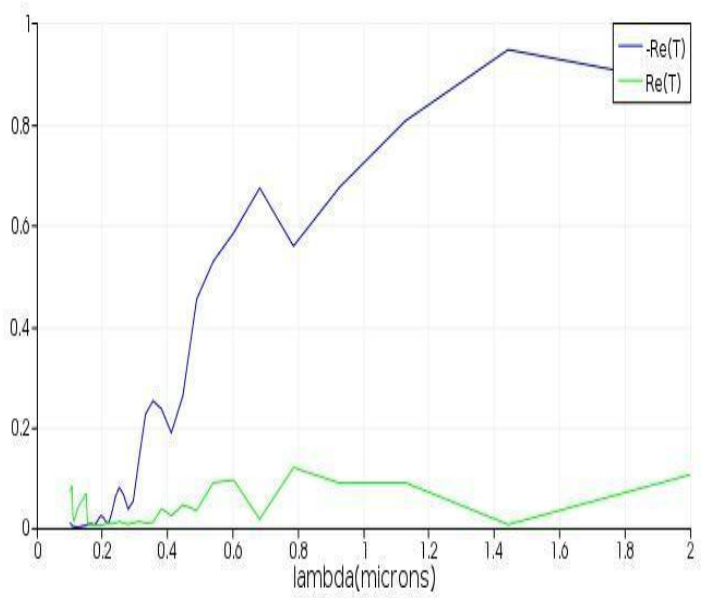

Figure (12) shows the reflection and transmission of the envelope after increasing the height to 245 nm.

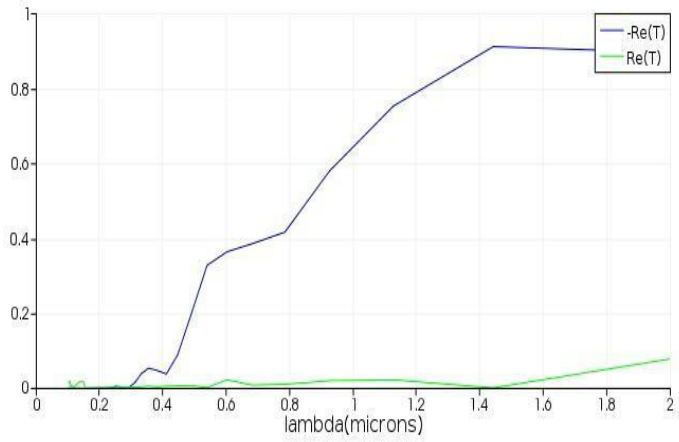

Figure (13) shows the reflection and transmission of the envelope after increasing the height to 490 nm.

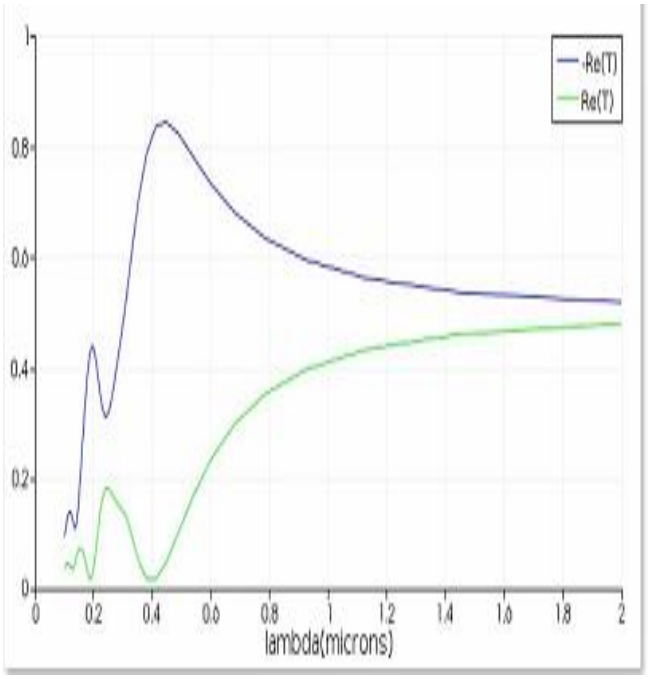

Figure (14) shows the transmission and reflection upon changing the envelope to a negative cosine (the taller domes are at the edges and the shorter one is in the middle).

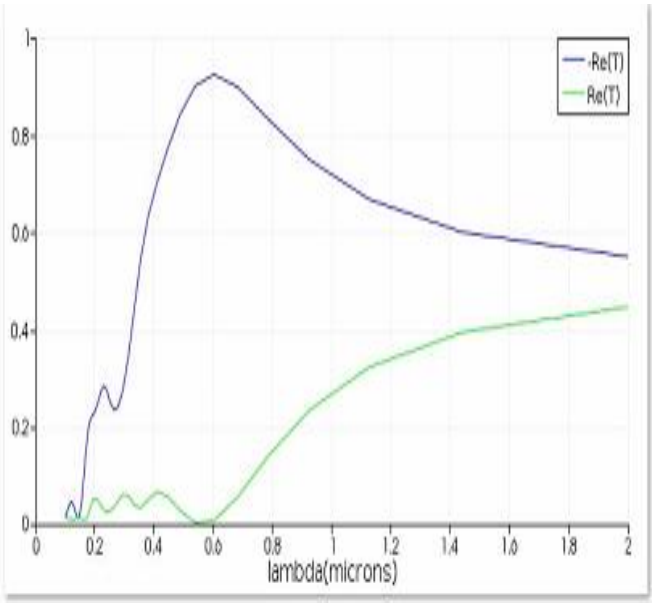

Figure (15) shows the reflection and transmission of a moth-eye structure of the same height of the individual domes as the one in the previous figure, but the envelope is a positive cosine function.

II) Number of Domes/ Envelope:

In this step, we increased the number of domes per envelope to investigate if this would be guiding the light more gradually and thus would minimize the reflection even more.

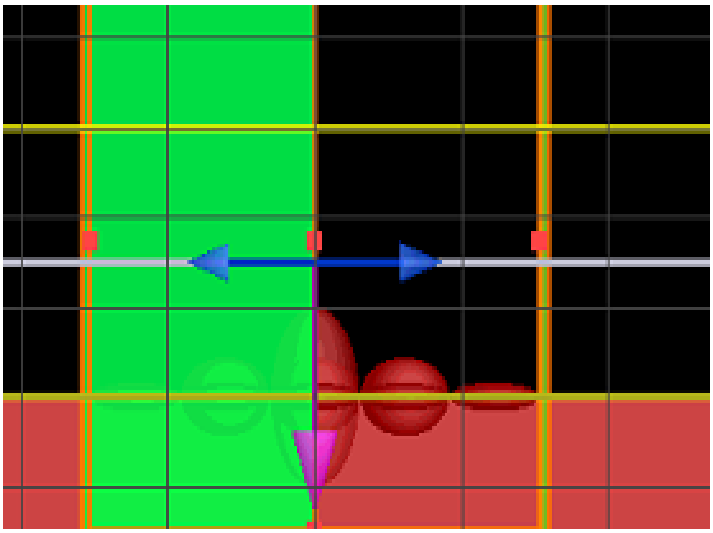

Figure (16) shows the structure upon increasing the number of domes/envelopes.

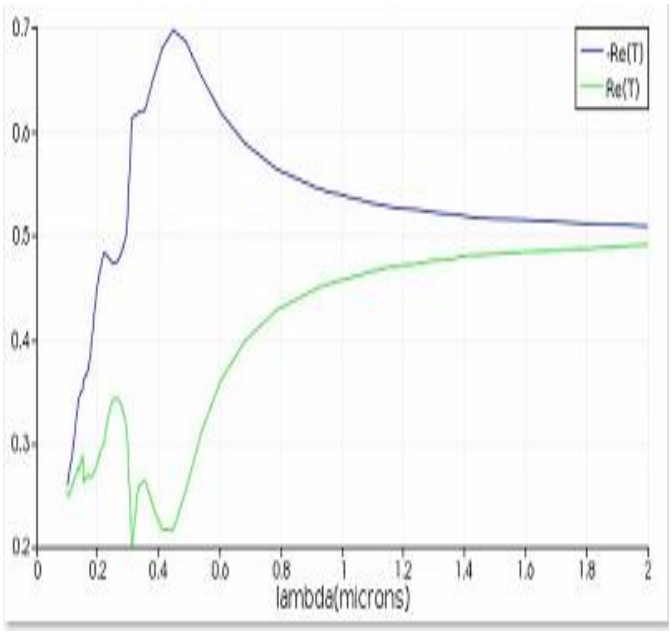

Figure (17) shows the reflection and transmission of a moth-eye structure with 5 domes/ envelope.

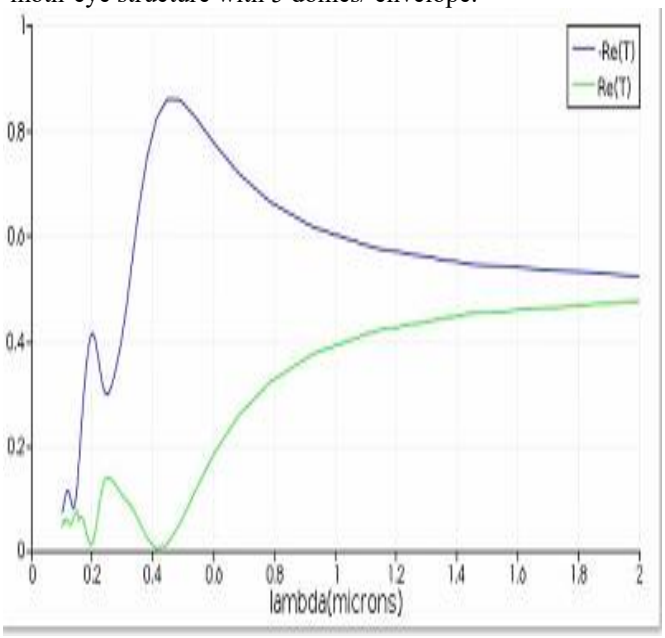

Figure (18) shows the reflection and transmission of a moth eye structure having 3 domes/envelope.

III) Relative heights of the domes:
In this step, relative heights of the domes were varied. This departs from the theory of self-similarity assumed before, but it aids in our objective of exhausting optimization approaches.

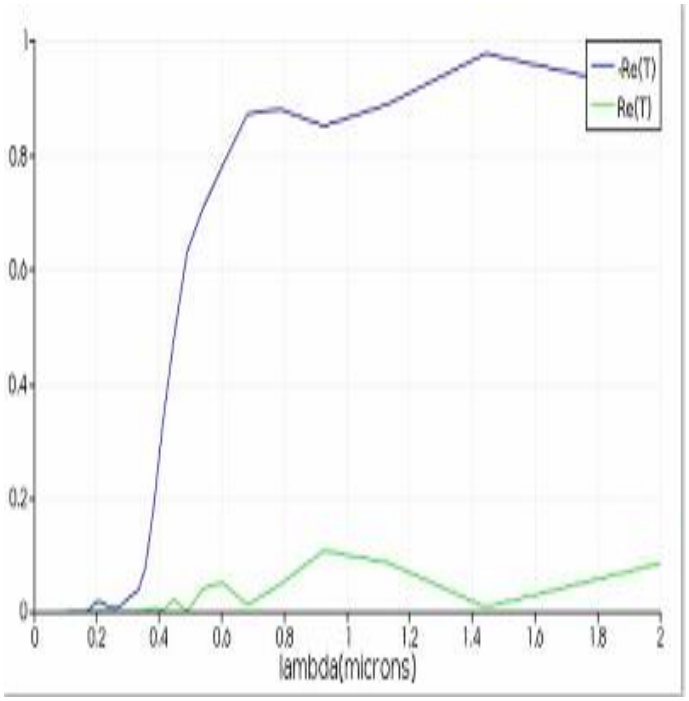

Figure (19) shows the reflection and transmission of the self-similar structure.

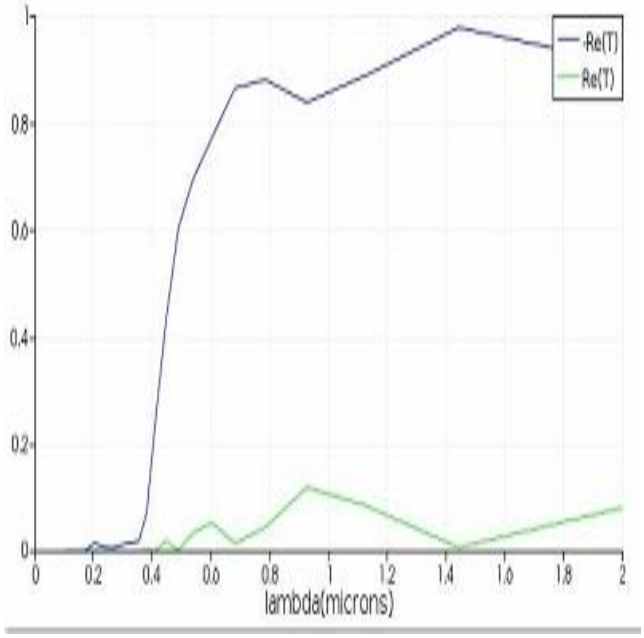

Figure (20) shows the transmission and reflection obtained upon increasing the relative heights to be 1.5 that in the previous figure of an ordinary self-similar structure.

IV) Separation of the Domes:

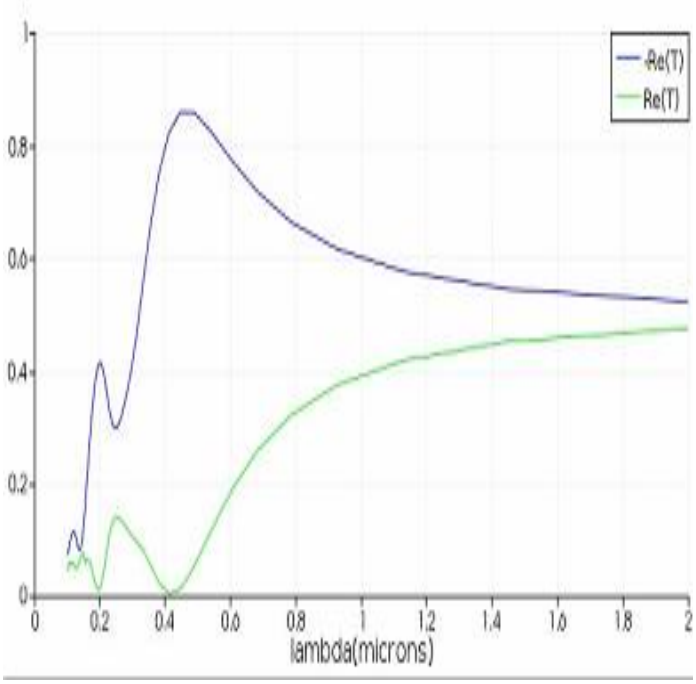

Figure (21) shows the reflection and transmission of domes with 1 nm separation.

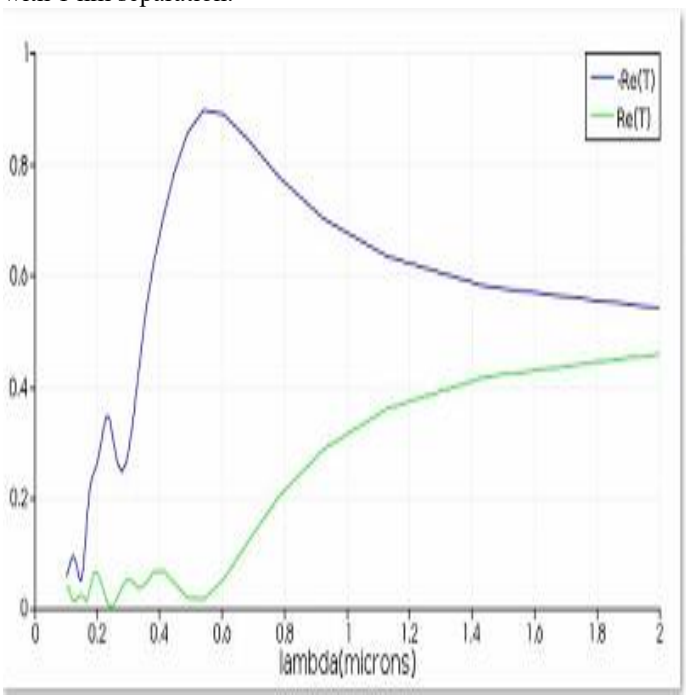

Figure (22) shows the reflection and transmission of domes with 5 nm separation.

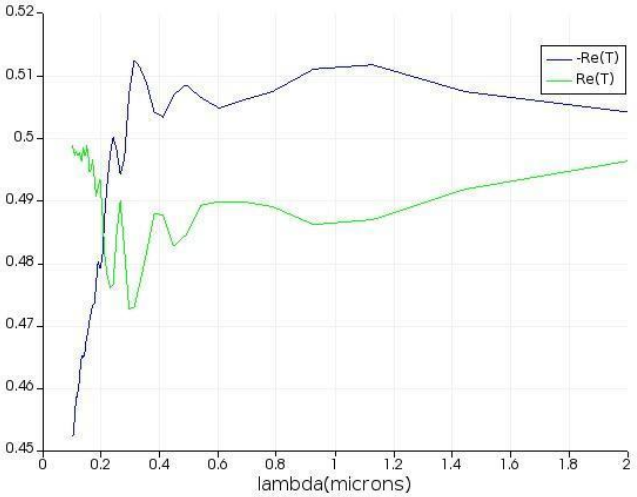

Figure (23) shows the reflection and transmission of domes with 980 nm separation.

V) Radius of each dome:

In this step, the radius of each dome increased keeping the separation distance the same- to investigate the effect of coating material preparation and application alone, which would help guide its synthesis.

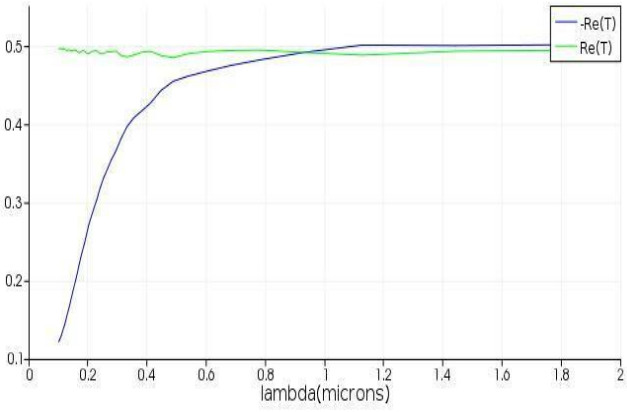

Figure (24) shows the reflection and transmission of the self-similar structure upon increasing the radius of each dome to 490 nm.

VI) Optimization: Complete Departure from Self-Similarity:

In this section, we further looked into a deeper conceptual basis controlling the reflection based on the previous trials. In this step, the rate of frequency of change of the relative heights is assumed to give the maximum antireflection and the theory is verified.

This principle is illustrated in the 2 figures below.

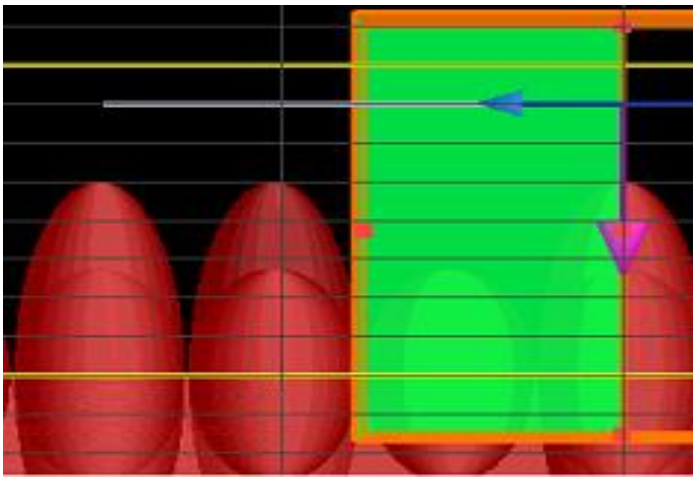

Figure (25) shows the effect of increasing the rate of the frequency of change of relative heights of the domes.

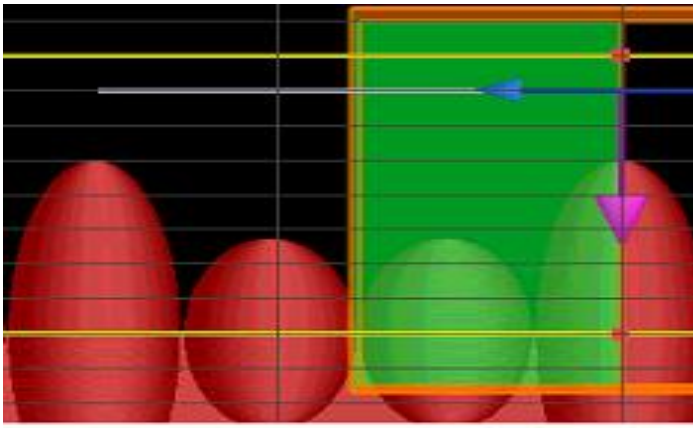

Figure (26) shows a typical self-similar structure as assumed.

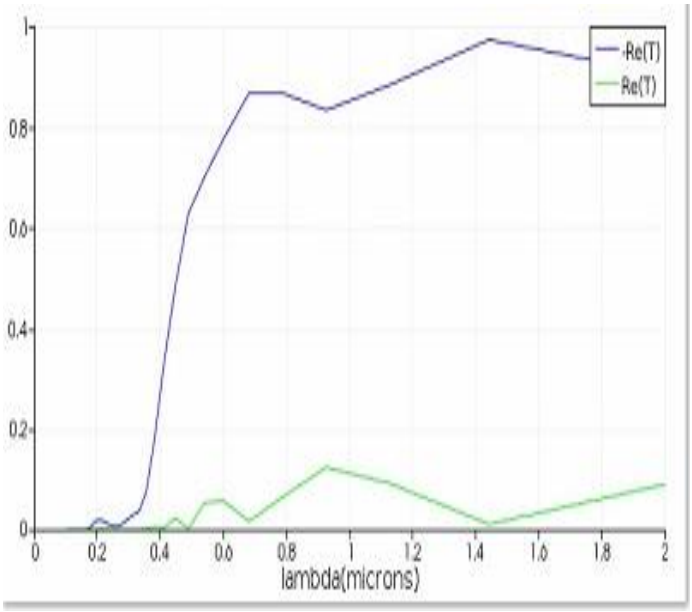

Figure (27) shows the optimum reflection and transmission attained for a self-similar structure of optimum height and other parameters.

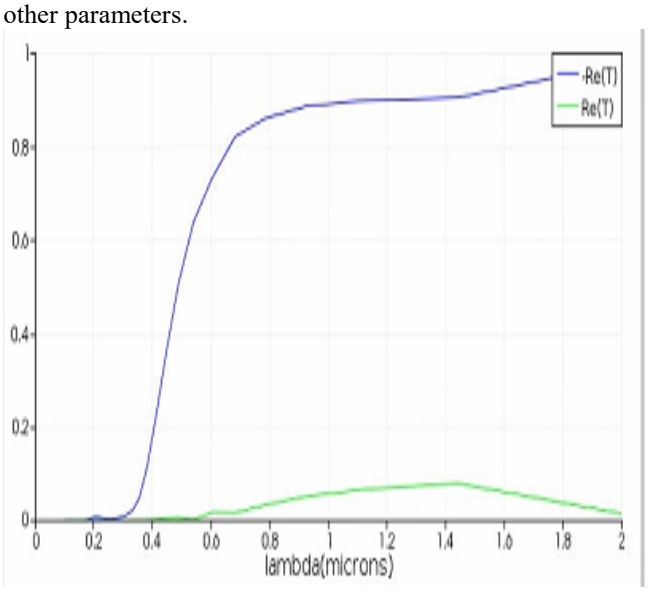

Figure (28) shows the effect of increasing the rate of individual and composite morphology change.

III. DISCUSSION:

Despite the conventional Rayleigh's explanation of graded refractive index and the predicted effect on the gradual change of the surface morphology that will guide the light into the surface below the textured layer, the numerical studies shown have disproved this. Thus, the basic concept upon which we built the first mathematical model (figure (1)), that is implemented in figure (2), was disproved as shown in multiple results. This is evident in the reflectivity of the self similar (SS) structure shown in figure (6), that is almost the same as the small structures (carrier cosine) reflectivity. Had the concept of increased confinement of light due to gradual change in the surface texturing been true, the self similar structure would have increased the reflectivity of both structures. Yet this hints to the significance of the role of the small structures, which could be referred to as hint (1).

Second, figures (7-13) show that increasing the height of these protrusions, which consequently decreases the gradual change in the surface, results in an enhanced transmission. This is another disproof of the conventional concept referred to. This also hints to the potential influence of increasing the height, referred to as hint (2)

Third, one can notice that perceiving the concept of self similarity as a negative cosine envelope for the carrier cosine shown in figure (1) would reach the utmost gradual change in the surface and would be the most clear cut decisive criterion to judge the validity of Rayleigh's prediction. Indeed, figures (14) and (15) are one more dispoof of this principle because of the higher reflectivity it shows especially in the VIS-UV band.

Fourth, if anyone would further refute this claim by suggesting that 3 domes (carrier cosine peaks) per envelope is a quite low level of self similarity, then the best counter-refutation is exploring the effect of a higher frequency carrier wave, which introduces more gradual change in the surface. This was further implemented in figure (16) and the results shown in figures (17) and (18) even tells that increasing that gradual change increases the reflectivity, specially in the UV band.

Fifth, one more possible counterclaim defending Rayleigh's principle could be suggesting changing the relative heights of the carrier cosine peaks per envelope (i.e., changing the envelope so that it does not follow a perfect cosine function). This is what was explored and whose results are shown in figure (19) that show no difference from figure (20), whose envelope follows a perfect cosine behavior.

Sixth, increasing separation between the domes decreases the gradual change in the surface. Figure (22) that increased the separation to 5 nm shows an increased transmission as compared to figure (21) of 1 nm separation, which are all far below the excitation wavelength. This is another clear contradiction to Rayleigh's principle. However, increasing it even more as shown in figure (23) to be exactly the same as the excitation wavelength increases the reflection in the UV band. However, it is important to note that this would then take it to the extreme of a flat surface. Thus, neither is Rayleigh's principle of gradual change nor the flat surface behavior or (even a closer tendency to this behavior) would increase the anti reflectivity, which is referred to as hint (3).

Exhausting all possible defenses to Rayleigh's principle that scientists can think of, we included one more seventh counterclaim, which is the influence of increasing the radius of each dome, which is a crystal clear increase in the gradual change of the surface. Figure (24) shows that this led to increasing the reflection, which is a seventh decisive disproof for Rayleigh's principle.

Based on all of such exhaustive parametric study results, comparisons, analyses and conclusions, we noticed that increasing the second order change in the vertical spatial variation with respect to the horizontal spatial axis of the interface below the textured surface increases the transmission. This is the pattern that controls the idea of surface texturing. Looking at it differently, the more abrupt the vertical change with respect to the horizontal surface expansion in the cross section front view, the more the anti-reflectivity. On that basis, we optimized the parameters to yield figures (27) and (28) having the best anti-reflective behavior, which would then need to be practically verified in another work.

IV. CONCLUSION:

The conventional theory of increasing light confinement through a gradual refractive index change induced by the gradual surface variation has been disproved based on seven clear-cut parametric study results and analyses. Then, novel observations on the underlying pattern maximizing the broadband antireflectivity was hypothesized and numerically verified. Despite that it has been numerically verified in multiple materials including polymers, glasses, and other dielectrics, to prove its independence on the material choice, the results of only one material was published here to avoid a large paper size.

V. ACKNOWLEDGMENT

First and foremost, thanks God, the supporter of every single step in that project. Second, I would like to thank Dr. I. Elsherbiny, Dr. M. Kandeel, Dr. M. Hussein, my friend S. Saeed, Dr. M. Saleh, Dr. I. Y. Zahran, Dr. M. Rashad, Dr. A. Mohammad, Dr. BA Anis, and every single person who provided any sort of advice, recommendation, financial support or permission to use his/her lab resources.

VI. CONFLICT OF INTERESTS

The authors declare no conflict of interests

REFERENCES

[1] Aboqara N., (2021), Unprecedented, Exhaustive Review and Roadmap for Upconverting Nanoparticles Field Enhancement Mechanisms to be utilized in Biomedical Applications

[2] Aboqara N. (2021), Unprecedented, Verified Roadmap for Material-Dependent Field Enhancement of Lanthanide Doped Upconverters to be utilized in Biomedical Applications

[3] Chen, Q., Hubbard, G., Shields, P. A., Liu, C., Allsopp, D. W., Wang, W. N., & Abbott, S. (2009). Broadband moth-eye antireflection coatings fabricated by low-cost nanoimprinting. *Applied Physics Letters*, *94*(26), 263118.

[4] Galeotti, F., Trespidi, F., Timò, G., & Pasini, M. (2014). Broadband and crack-free antireflection coatings by self-assembled moth eye patterns. *ACS applied materials & interfaces*, *6*(8), 5827-5834.

[5] Tommila, J., Aho, A., Tukiainen, A., Polojärvi, V., Salmi, J., Niemi, T., & Guina, M. (2013). Moth-eye antireflection coating fabricated by nanoimprint lithography on 1 eV dilute nitride solar cell. *Progress in Photovoltaics: Research and Applications*, *21*(5), 1158-1162.

[6] Brinker, C. J., & Hurd, A. J. (1994). Fundamentals of sol-gel dip-coating. *Journal de Physique III*, *4*(7), 1231-1242.

[7] Walheim, S., Schäffer, E., Mlynek, J., & Steiner, U. (1999). Nanophase-separated polymer films as high-

performance antireflection coatings. *Science*, *283*(5401), 520-522.

[9] Tait, R. N., Smy, T., & Brett, M. J. (1993). Modelling and characterization of columnar growth in evaporated films. *Thin Solid Films*, *226*(2), 196-201.

[10] Kennedy, S. R., & Brett, M. J. (2003). Porous broadband antireflection coating by glancing angle deposition. *Applied optics*, *42*(22), 4573-4579.

[11] Raut, H. K., Ganesh, V. A., Nair, A. S., & Ramakrishna, S. (2011). Anti-reflective coatings: A critical, in-depth review. *Energy & Environmental Science*, *4*(10), 3779-3804.

[12] Forberich, K., Dennler, G., Scharber, M. C., Hingerl, K., Fromherz, T., & Brabec, C. J. (2008). Performance improvement of organic solar cells with moth eye anti-reflection coating. *Thin Solid Films*, *516*(20), 7167-7170.

[13] Glaser, T., Ihring, A., Morgenroth, W., Seifert, N., Schröter, S., & Baier, V. (2005). High temperature resistant antireflective moth-eye structures for infrared radiation sensors. *Microsystem technologies*, *11*(2-3), 86-90.

[14] Cui, H., Pillai, S., Campbell, P., & Green, M. (2013). A novel silver nanoparticle assisted texture as broadband antireflection coating for solar cell applications. *Solar Energy Materials and Solar Cells*, *109*, 233-239.

[15] Shin, B. K., Lee, T. I., Xiong, J., Hwang, C., Noh, G., Cho, J. H., & Myoung, J. M. (2011). Bottom-up grown ZnO nanorods for an antireflective moth-eye structure on CuInGaSe2 solar cells. *Solar energy materials and solar cells*, *95*(9), 2650-2654.

[16] Chen, J. Y., Chang, W. L., Huang, C. K., & Sun, K. W. (2011). Biomimetic nanostructured antireflection coating and its application on crystalline silicon solar cells. *Optics express*, *19*(15), 14411-14419.

[17] Boden, S. A., & Bagnall, D. M. (2010). Optimization of moth-eye antireflection schemes for silicon solar cells. *Progress in Photovoltaics: Research and Applications*, *18*(3), 195-203.

[18] Ji, S., Song, K., Nguyen, T. B., Kim, N., & Lim, H. (2013). Optimal moth eye nanostructure array on transparent glass towards broadband antireflection. *ACS applied materials & interfaces*, *5*(21), 10731-10737.

[19] Yamada, N., Kim, O. N., Tokimitsu, T., Nakai, Y., & Masuda, H. (2011). Optimization of anti-reflection moth-eye structures for use in crystalline silicon solar cells. *Progress in Photovoltaics: Research and Applications*, *19*(2), 134-140.

[20] Khezripour, Z., Mahani, F. F., & Mokhtari, A. (2018, March). Optimized design of silicon-based moth eye nanostructures for thin film solar cells. In *2018 3rd Conference on Swarm Intelligence and Evolutionary Computation (CSIEC)* (pp. 1-4). IEEE.

[21] Shen, L., Du, H., Yang, J., & Ma, Z. (2015). Optimized broad band and quasi-omnidirectional anti-reflection properties with moth-eye structures by low cost replica molding. *Applied Surface Science*, *325*, 100-104.

[22] JosephWeiblen, R., Florea, C., Docherty, A., Menyuk, C. R., Shaw, B., Sanghera, J., ... & Aggarwal, I. (2012, September). Optimizing motheye antireflective structures for maximum coupling through As 2 S 3 optical fibers. In *IEEE Photonics Conference 2012* (pp. 824-825). IEEE.

[23] Choi, J. S., An, J. H., Lee, J. K., Lee, J. Y., & Kang, S. M. (2020). Optimization of Shapes and Sizes of Moth-Eye-Inspired Structures for the Enhancement of Their Antireflective Properties. *Polymers*, *12*(2), 296.

[24] Raut, H. K., Ganesh, V. A., Nair, A. S., & Ramakrishna, S. (2011). Anti-reflective coatings: A critical, in-depth review. *Energy & Environmental Science*, *4*(10), 3779-3804.

[25] Zhou, C., & Troian, S. M. (2018). Self-Similar Cusp Formation in Thin Liquid Films By Runaway Thermocapillary Forces. *arXiv preprint arXiv:1808.01017*.

[26] Fan, P., Bai, B., Jin, G., Zhang, H., & Zhong, M. (2018). Patternable fabrication of hyper-hierarchical metal surface structures for ultrabroadband antireflection and self-cleaning. *Applied Surface Science*, *457*, 991-999.

[27] Won, S. H. (2015). Omni-directional Broadband Antireflection coating for solar cells using Indium Tin Oxide (ITO) based Fractal Structures.